Pis'ma v ZhETF, vol. 101, iss. 4, pp. 240 – 245 © 2015 February 25

Calculation of QCD parameters by using the jet resolution parameter

R. Saleh-Moghaddam[1)], *M. E. Zomorrodian*[*)]

Department of Physics, Faculty of sciences, Ferdowsi University of Mashhad, 91775-1436 Mashhad, Iran

Submitted 22 December 2014

We describe the measurement of the coupling constant from both the dispersive and the shape function models. This parameter depends on the scale at which the QCD process occurs. We present distributions of the jet resolution parameter (Y_3). This parameter is one observable among the event shape variables. Both models are divided into the perturbative as well as the non-perturbative regions. The average value of the strong coupling constant is $\alpha_s = 0.11887 \pm 0.03537$ being consistent with world average. We will explain all these features in this paper.

DOI: 10.7868/S0370274X15040025

I. Introduction. The ultimate goal of research in high-energy physics is to understand and describe the structure of matter and its interactions. There are four known forces governing our world: gravitational, weak, electromagnetic, and strong. Only the last three play a major role in the microscopic world. In the modern language of physics, interactions are due to exchange of field quanta that determine the properties of these interactions. The interactions of quarks and gluons are described by quantum chromo dynamics (QCD), a non-abelian gauge theory based on the SU (3) color symmetry group. Color constitutes the equivalent of the electric charge in electromagnetic interactions. The effective strong coupling constant as depends on the scale at which the QCD process occurs. The solution of the renormalization group equation in leading order leads to:

$$\alpha_s(Q^2) = \frac{4\pi}{\beta_0 \ln(Q^2/\Lambda^2)}, \qquad (1)$$

where Q^2 denotes the scale at which as is probed and Λ is a QCD cutoff parameter. The parameter $\beta_0 = = 11 - (2/3)N_f$ depends on the number of quark flavors (N_f) in the theory. Since the known number of flavors is six, $\beta_0 > 0$, and the coupling constant becomes smaller the larger the scale Q^2. The property of asymptotic freedom has been proven rigorously and allows us to make predictions for the properties of strong interactions in the perturbative QCD regime, in which as is small.

Quantum chromo dynamics has two properties that make it much more difficult to work with theoretically than electroweak theory. The first property is that the coupling constant is large, making the use of perturbation theory difficult. The strong coupling constant depends on the scale, as described above, and cross sections can be calculated only for scatterings with a hard scale, for which as is small enough. The second property is the non-abelian nature of the interaction. Gluons can interact with other gluons, leading to confinement of color [1].

The description of e^+e^- annihilation into hadronic events involves a number of components: the E_{cm} dependence of the total cross section and flavor composition, multi parton matrix elements, angular orientation of events, initial-state photon bremsstrahlung and effects of initial-state electron polarization [2].

The aim of the present investigation is to justify the measure of the coupling constant in perturbative as well as in nonperturbative theory by using the jet resolution parameter as an event shape observable explained in Section II. We define the power corrections in Section III. Then we calculate the strong coupling constant and the nonperturbative parameter by using the NLO (Next-to-Leading Order) and NNLO (Next to Next to Leading Order) corrections followed by the Dispersive model and the Shape function model in Section IV. Section 5 summarizes our conclusions.

II. The jet resolution parameters. In this section we study the jet resolution parameters as an event shape variable. Event shape observables measure geometrical properties of hadronic final states at high energy particle collisions. They have been studied at e^+e^- collider experiments. Apart from distributions of these observables, we will also study the mean values as well as the higher orders of the moments of event shape observables.

The jet resolution parameters y_n are defined as the particular values of $y_{\rm cut}$ at which an event changes from a $(n-1)$-jet configuration to a n-jet configuration. The same clustering algorithm as for jet rates is applied [3].

[1)]e-mail: R_Saleh88@yahoo.com; Zomorrod@um.ac.ir

We propose using the Durham algorithm ($k_\perp$ algorithm) for jets produced in the deep inelastic hadron scattering process. On the theoretical side this implies the presence of large order corrections that cannot be resumed; on the experimental side the trouble is that ghost jets may appear, i.e., jets along directions where no particles are present. To cure this problem the Durham algorithm was introduced, which is based on the following definition of the test variable [4]. The following distance measures are used for Durham algorithm for every pair of hadrons h_k and h_l compute the corresponding relative transverse momentum:

$$y_{kl} = \frac{2\min(E_k^2, E_l^2)(1-\cos\theta_{kl})}{E_{\rm vis}^2}, \qquad (2)$$

where E_k and E_l denote the energy of the final-state, by θ_{kl} the angle between the momenta of hadrons. Take the smallest value among E_k^2 and E_l^2. If y_{ij} is the smallest value y_{kl} computed and $y_{kl} \leq y_{\rm cut}$ combine (P_i, P_j) into a single pre-cluster (pseudo particle) $P_{ij} = P_i + P_j$ according to a recombination prescription. For resolving jet structure, we define a resolution parameter $y_{\rm cut} = Q_0^2/E_{\rm vis}^2 \leqslant 1$. Repeat this procedure until all pairs of objects (particle and/or pseudo particles) have $y_{kl} \geqslant y_{\rm cut}$. Whatever objects remain at this stage are called jets (k algorithm). Clearly the resolution criterion $y_{kl}^D \geqslant y_{\rm cut}$ becomes, for small angles, $k_{Tk}^2 \geqslant E_{\rm vis}^2 y_{\rm cut}$, where k_{Tk} is the transverse momentum of the k-th particle to the direction of the l-th one. In this way the algorithm tries to minimize the transverse momentum and not the invariant mass. On the other hand the recombination scheme is still given by P_{ij} [4, 5]. In this article, we use y_{23}^D variable, which we call y_3. Now we present power corrections for this event shape variable. By using the power correction, we can calculate the coupling constants in the perturbative and in the nonperturbative part of theory.

III. Power corrections. The n-th moment of an event shape observable y is defined by:

$$\langle y^n\rangle = \int_0^{y_{\max}} y^n \frac{1}{\sigma_{\rm had}}\frac{d\sigma}{dy}dy, \qquad (3)$$

$y_{\max}$ is the kinematically allowed upper limit of the observable [6]. By naively neglecting the integration over the unphysical range of negative variable values, we obtain:

$$\langle y^n\rangle = \int_0^{y_{\max}} y^n \frac{1}{\sigma_{\rm had}}\frac{d\sigma}{dy}dy = \\ = \int_{-a_y P}^{y_{\max}-a_y P} (y+a_y P)^n \frac{1}{\sigma_{\rm had}}\frac{d\sigma_{pt}}{dy}dy. \qquad (4)$$

Discarding the integration over the kinematically forbidden values of y. This leads to the nonperturbative predictions. The prediction for the moment on hadron level will be [7]:

$$\langle y^1\rangle = \langle y^1\rangle_{\rm NLO} + a_y P, \qquad (5)$$

$$\langle y^2\rangle = \langle y^2\rangle_{\rm NLO} + 2\langle y^1\rangle_{\rm NLO}(a_y P) + (a_y P)^2, \qquad (6)$$

$$\langle y^3\rangle = \langle y^3\rangle_{\rm NLO} + 3\langle y^2\rangle_{\rm NLO}(a_y P) + \\ + 3\langle y^1\rangle_{\rm NLO}(a_y P)^2 + (a_y P)^3, \qquad (7)$$

$$\langle y^4\rangle = \langle y^4\rangle_{\rm NLO} + 4\langle y^3\rangle_{\rm NLO}(a_y P) + \\ + 6\langle y^2\rangle_{\rm NLO}(a_y P)^2 + 4\langle y^1\rangle_{\rm NLO}(a_y P)^3 + (a_y P)^4, \qquad (8)$$

$$\langle y^5\rangle = \langle y^5\rangle_{\rm NLO} + 5\langle y^4\rangle_{\rm NLO}(a_y P) + 10\langle y^3\rangle_{\rm NLO}(a_y P)^2 + \\ + 10\langle y^2\rangle_{\rm NLO}(a_y P)^3 + 5\langle y^1\rangle_{\rm NLO}(a_y P)^4 + (a_y P)^5. \qquad (9)$$

IV. Measurements of coupling constants. The QCD running of α_s implies that the effective coupling $\alpha_s(Q)$ is small at high energy Q. This property justifies the use of perturbation theory for predicting jet observables, at least at asymptotic energies. Measurements of the strong coupling constant (α_s) are obtained by different observables, and different analysis methods serve as an important consistency test of QCD. α_s is measured at a given scale, QCD predicts its energy dependence as described by the renormalization group equation [7]. A coupling constant is a number that determines the strength of the force exerted in an interaction. For electromagnetism, the coupling constant is related to the electric charge through the fine structure constant. If the coupling constant gets very large compared to unity, perturbation theory becomes useless, because higher powers of the expansion parameter are bigger, not smaller, than lower powers. This is called a strongly coupled theory. Coupling constants in quantum field theory end up depending on energy because of quantum vacuum effects. A quantum field theory can be weakly coupled at low energies and strongly coupled at high energies, as is true with the fine structure constant a in QED, or strongly coupled at low energies and weakly coupled at high energies, as is true with the coupling constant for quark and gluon interactions in QCD.

The analytical power ansatz for nonperturbative corrections by Dokshitzer and Webber [8, 9] including the Milan factor established by Dokshitzer [10, 11] is used to determine α_s from mean event shapes. This ansatz provides an additive term to the perturbative $O(\alpha_s^2)$ QCD prediction [12]:

$$\langle y\rangle = \langle y^{\rm pert}\rangle + \langle y^{\rm pow}\rangle = \frac{1}{\sigma_{\rm tot}}\int y\frac{dy}{d\sigma}d\sigma. \qquad (10)$$

In the following we calculate the strong coupling constant in perturbative region as well as the nonperturbative parameters by using different models.

Calculations in perturbative QCD have been found to give fairly accurate descriptions of cross sections up to Next-to-Leading Order for a lot of different reactions. The next step to a complete comprehension of QCD is the understanding of the non-perturbative parts.

Perturbative QCD is (and continues to be) well tested, and QCD studies have entered the precision era, i.e. experiments are sensitive to genuine Quantum Field Theory effects. Each order in the perturbative series in helps to increase the reliability of QCD predictions. Next-to-Leading Order theory includes only the perturbative theory. The mean value of the jet resolution variable as an event shape observable in the perturbative prediction is:

$$\langle Y_3^{\rm pert}\rangle = \overline{A}_f \frac{\alpha_s(\mu)}{2\pi} + \left(\overline{B}_f + \overline{A}_f\,\beta_0 \log\frac{\mu^2}{Q^2}\right)\left[\frac{\alpha_s(\mu)}{2\pi}\right]^2, \tag{11}$$

where $\overline{A}_f = A_f$, $\overline{B}_f = B_f - \frac{3}{2}C_A A_f$, $\beta_0 = (33 - -2N_f)/12\pi$, and μ being the renormalization scale. The coefficient A_f and B_f were determined from the $O(\alpha_s^2)$ perturbative calculations [13]. And the numerical values of these coefficients are tabulated in [14]. Quantum chromo dynamics color factors are:

$$C_A = 3,\ C_F = \frac{N^2-1}{2N} = \frac{4}{3} \tag{12}$$

for $N = 3$ color quarks.

The above expansion can be including the next order. This expansion told the next to next to leading order. Consequently the Eq. (11) changes to the following expansion:

$$\langle Y_3^{\rm pert}\rangle = \overline{A}_f \frac{\alpha_s(\mu)}{2\pi} + \left(\overline{B}_f + \overline{A}_f \beta_0 \log\frac{\mu^2}{Q^2}\right)\left[\frac{\alpha_s(\mu)}{2\pi}\right]^2 + \\ + \left[\overline{C}_f + 2\overline{B}_f\beta_0 \log\frac{\mu^2}{Q^2} + \overline{A}_f\left(\beta_0^2 \log^2\frac{\mu^2}{Q^2} + \right.\right. \\ \left.\left. + \beta_1 \log\frac{\mu^2}{Q^2}\right)\right]\left[\frac{\alpha_s(\mu)}{2\pi}\right]^3 + O(\alpha_s^4). \tag{13}$$

A. The dispersive model. The dispersive model gives predictions for several observables and contains only universal free parameters. Opposite to our previous model, this model includes both perturbative region and nonperturbative part of theory. It calculates the strong coupling constant $\alpha_s(M_{Z^0})$ and the nonperturbative constant $\alpha_0(\mu_I)$.

The perturbative constant is obtained from Eq. (11) and the nonperturbative is given by:

$$\langle y^{\rm pow}\rangle = a_y P = a_y \frac{4C_F}{\pi^2} M \frac{\mu_I}{Q} \times \\ \times\left[\alpha_0(\mu_I)\alpha_s(\mu_I) - \left(\log\frac{\mu}{\mu_I} + 1 + \frac{k}{4\pi\beta_0}\right)\cdot 2\beta_0\alpha_0^2(\mu_I)\right]. \tag{14}$$

where α_0 is a nonperturbative parameter accounting for the contributions to the event shape below an infrared matching scale $\mu_I \cong 2$. In the ($\overline{MS}$) renormalization scheme the constant k has the value $k = = (\frac{67}{18} - \frac{\pi^2}{6})C_A - \frac{5}{9}N_f$, with $N_f = 5$ at the studied energies. The Milan Factor M is known in two loops $M = 1.49 \pm 0.20$ [10, 15].

We are using in this analysis the simulated hadron data: Monte Carlo (MC: PYTHIA program) as well as the DELPHI and OPAL experimental data to calculate the strong coupling constant in perturbative theory for different power corrections. The reason behind this is to see if there are any differences between the lower and the higher order moments.

Fig. 1 shows the mean value of the jet resolution parameter $\langle Y_3\rangle$ up to the fifth order for the power corrections as a function of the center of mass energy fitted to the NLO and NNLO corrections. We also display the mean value of the jet resolution variable fitted to the Dispersive model. The figure indicates that the results obtained from the DELPHI and OPAL data coincide well within the statistical errors to those obtained from the MC data. So according to this agreement, we have made a single fitting procedure to MC data. We observe the more agreement between the theory and experiment as the order of the power correction increases.

By fitting the dispersive model with the available data, we calculate the strong coupling constant (α_S) together with the non-perturbative parameter (α_0). We observe more agreement between this model with the data than the NNLO predictions. Also there is more consistency as the order of the power corrections increases. The reason is that the dispersive model includes both perturbative and the non-perturbative parts of the QCD calculation, while the NNLO just includes the perturbative part of the theory. Our results for α_s and α_0 are tabulated in Tables I and II respectively.

A decrease in the value of the coupling constants is quite visible by increasing the order of the power correction. We conclude that the coupling constant becomes more consistent with the theoretical value by increasing the order of the power corrections. Also the obtained values are consistent with other event shape variables [14] and QCD predictions [16]. The errors cited in the table are statistical only.

B. The shape function model. Korchemsky and Tafat [17] describe properties of the event shape variables which are not included in NLO perturbation theory by a so called shape function, and do not depend on the vari-

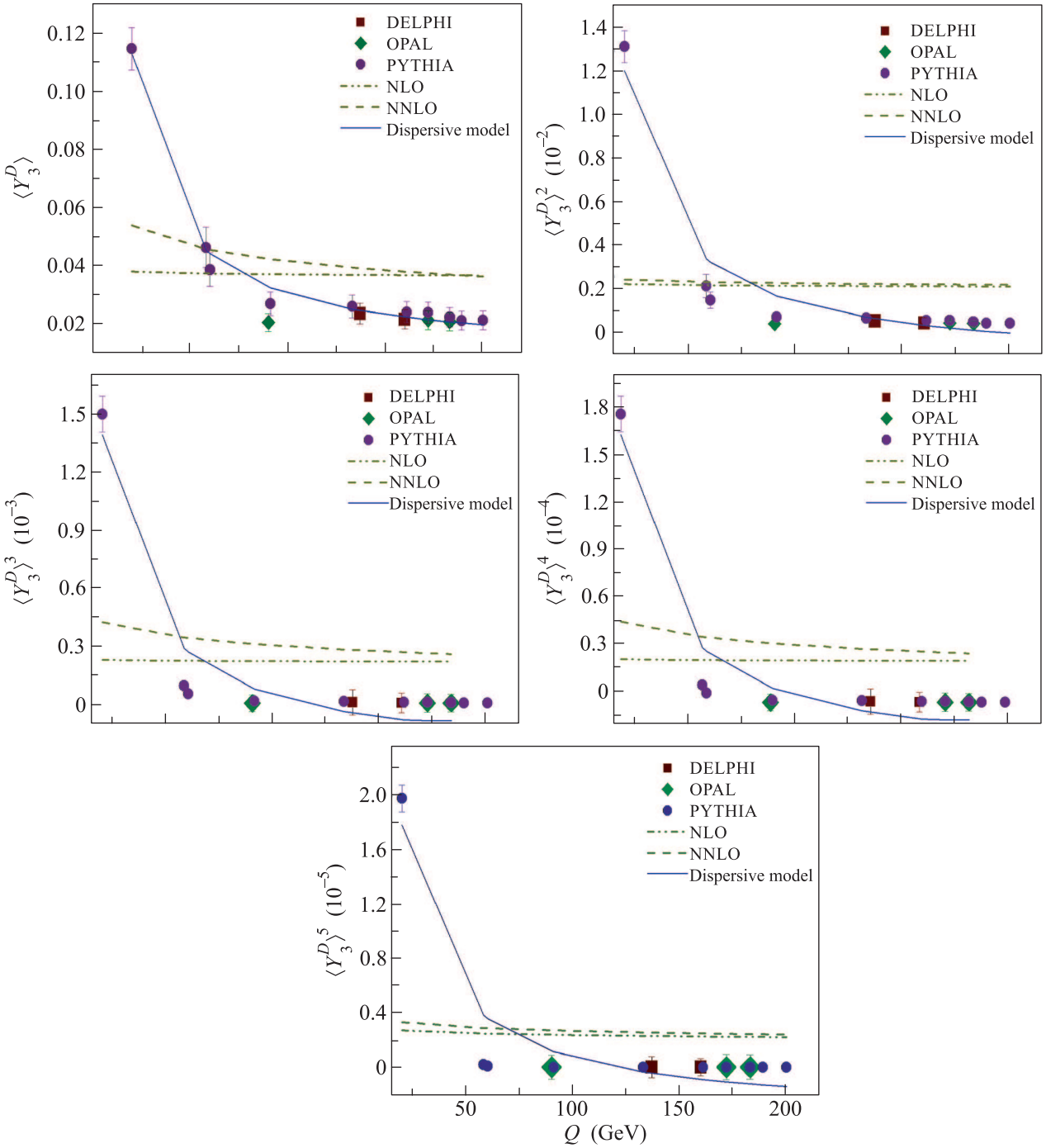

Fig. 1. Fits of the Dispersive model and NLO and NNLO moments up to fifth order

able nor the centre of mass energy. This is more general than the dispersive model, considering both as a shift of the perturbative prediction and as a compression of the distribution peak. The prediction is deduced from studying the two jet region in the distribution of the event shape variable y. The prediction for the differential distribution is:

$$\frac{1}{\sigma}\frac{d\sigma}{dy} = \int_0^{Q_y} d\varepsilon\, f_y(\varepsilon)\frac{d\sigma_{\mathrm{NLO}}}{dy}\left(y - \frac{\varepsilon}{Q}\right) \qquad (15)$$

with a non-perturbative function $f_y(\varepsilon)$, dependent on one scale parameter ε. This function is derived from the shape function $f(\varepsilon_L, \varepsilon_R)$ [15], which depends on two scale parameters $\varepsilon_L, \varepsilon_R$ for the two hemispheres of the

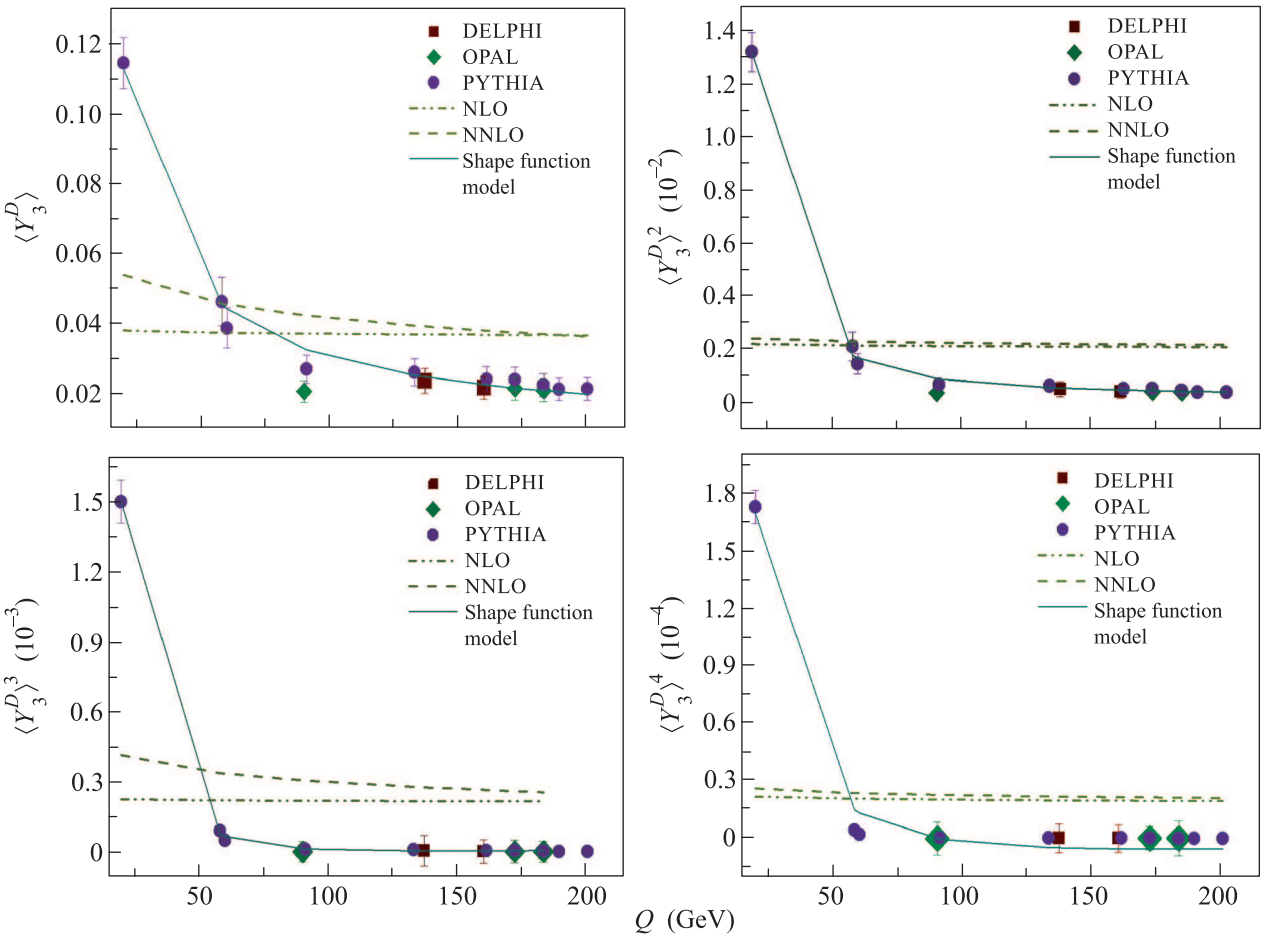

Fig. 2. Fits of the shape function model to PYTHIA data for $\langle (Y_3)^n \rangle$

event. By the compression of the distribution the validity of the prediction is extended compared to the dispersive model to $y \sim \Lambda_{\rm QCD}/Q$.

Table I

$\alpha_s(M_{Z^0})$ values of variable $\langle Y_3 \rangle$ for different orders

Event shape variables	$\alpha_s(M_{Z^0})$ (NLO)	$\alpha_s(M_{Z^0})$ (NNLO)
$\langle Y_3 \rangle^1$	0.1327 ± 0.02837	0.14545 ± 0.02256
$\langle Y_3 \rangle^2$	0.12935 ± 0.06056	0.13068 ± 0.05441
$\langle Y_3 \rangle^3$	0.11255 ± 0.04793	0.12029 ± 0.0501
$\langle Y_3 \rangle^4$	0.10557 ± 0.0610	0.10639 ± 0.0541
$\langle Y_3 \rangle^5$	0.10289 ± 0.04748	0.10411 ± 0.04086

Predictions for event shape variables in shape function model for non-perturbative parameters can be derived, λ_1 and λ_2 can also be obtained from fit to the data [16].

By using the relations for the distribution of the variables, we can calculate the mean values with respect to

Table II

$\alpha_0(\mu_I)$ values of variable $\langle Y_3 \rangle$ for different orders

Event shape variables	$\alpha_0(\mu_I)$
$\langle Y_3 \rangle^1$	0.58599 ± 0.0162
$\langle Y_3 \rangle^2$	0.57053 ± 0.04089
$\langle Y_3 \rangle^3$	0.56833 ± 0.0109
$\langle Y_3 \rangle^4$	0.56275 ± 0.01126
$\langle Y_3 \rangle^5$	0.557 ± 0.011393

non-perturbative distributions [17]. The shape function model gives predictions for several observables and contains only universal free parameters λ_1, λ_2 and $\alpha_s(M_{Z^0})$. In this section, we give the obtained results in the following:

$$\langle (Y_3)^1 \rangle = \langle (Y_3)^1 \rangle_{PT} + \frac{\lambda_1}{Q}. \qquad (16)$$

Analogously for the second moments, we find [16]:

$$\langle (Y_3)^2 \rangle = \langle (Y_3)^2 \rangle_{PT} + 2\frac{\lambda_1}{Q}\langle (Y_3)^1 \rangle_{PT} + \frac{\lambda_2}{Q^2}. \qquad (17)$$

Fig. 2 shows the mean value of $\langle Y_3 \rangle$ versus the center of mass energy for both Monte Carlo and the experimental data up to forth order. We observe that the shape function (solid line) follows the same trend as the results obtained from the data. In addition the obtained values extracted from the experimental data are consistent both with the Monte Carlo distribution and with the shape function model. On the other hand, if we compare our results with NNLO (dash line) and NLO (dot line) predictions, we come to a conclusion that the shape function model is in more agreement with the MC and the experimental data, than with the NLO prediction. The figure also indicates that there is an improvement as the order of the power correction increases.

By fitting the shape function model (Eqs. (11) and (16)) with the data, we obtain the values of the strong coupling constant (α_s) and the non-perturbative parameter (λ) up to the forth order. Our measured values are tabulated in Tables III for $\alpha_s(M_{Z^0})$. We observe that the mean value for our results in perturbative region is: $\alpha_s = 0.1163625 \pm 0.01369$. Also the obtained mean value in non-perturbative part of model is $\lambda = 1.48599 \pm 0.090688$.

We conclude that the results obtained from the above models conform well to the QCD prediction [16].

Table III

$\alpha_s(M_{Z^0})$ values of variable $\langle Y_3 \rangle$ for different orders

Event shape variables	$\alpha_s(M_{Z^0})$
$\langle Y_3 \rangle^1$	0.12802 ± 0.01322
$\langle Y_3 \rangle^2$	0.11536 ± 0.01703
$\langle Y_3 \rangle^3$	0.11368 ± 0.01172
$\langle Y_3 \rangle^4$	0.10839 ± 0.01277

This work was funded by vice president for research and technology of Ferdowsi University of Mashhad, Code 2/31742.

V. Conclusions. In this article we study the properties of QCD predictions for calculation of different parameters in this theory. We have calculated both the strong coupling constant (α_s) in perturbative and the free parameter in non-perturbative theories, by using the dispersive as well as the shape function models. To achieve this, the jet resolution parameter (as an event shape variable) is employed. We have also used the power corrections for our analyses. As we expected the NNLO predictions give us more accurate with the data than the NLO prediction. Having extracted the corresponding parameters (coupling constants) in perturbative and non-perturbative parts of theory for each model (by fitting the models with the experimental and Monte Carlo (PYTHIA) data), we obtained the strong coupling constant $\alpha_s = 0.1163625 \pm 0.01369$. Our obtained results are in a good agreement with the QCD theory.

1. H. Abramowicz and A. C. Caldwell, Rev. Mod. Phys. **71**, 5 (1999).
2. T. Sjostrand, S. Mrenna, and P. Skands, JHEP **05**, 026 (2006).
3. L3 Collaboration, PMC Physics A **2**, 6 (2008).
4. The ALEPH Collaboration, Eur. Phys. J. C **35**, 457 (2004).
5. L. Angelini, P. de Felice, M. Maggi, G. Nardulli, M. Pellicoro, and S. Stramaglia, Phys. Lett. B **545**, 315 (2002).
6. T. Gehrmann, M. Jaquier, and G. Luisoni, Eur. Phys. J. C **67**, 57 (2010).
7. S. Kluth, Arxiv:hep-ex/0505026v1 (2005).
8. Y. L. Dokshitzer and B. R. Webber, Phys. Lett. B **352**, 451 (1995).
9. B. R. Webber, arXiv: hep-ph/9510283 (1995).
10. Yu. L. Dokshitzer, A. Lucenti, G. Marchesini, and G. P. Salam, Nucl. Phys. B **511**, 396 (1998).
11. Yu. L. Dokshitzer, A. Lucenti, G. Marchesini, and G. P. Salam, JHEP **05**, 003 (1998); Arxiv: hep-ph/9802381.
12. J. Drees, U. Flagmeyer, K. Hamacher, O. Passon, R. Reinhardt and D. Wicke, *DELPHI Collaboration 99-19 CONF* 219 (1999).
13. A. Gehrmann-De Ridder, T. Gehrmann, E. W. N. Glover, and G. Heinrich, JHEP **05**, 106 (2009).
14. R. Saleh-Moghaddam and M. E. Zomorrodian, Pramana **81**(5), 775 (2013).
15. M. Dasgupta, L. Magnea, and G. Smye, J. High Energy Phys. **11**, 025 (1999).
16. C. Pahl, S. Bethke, O. Biebel, S. Kluth, and J. Schieck, Eur. Phys. J. C **64**, 533 (2009).
17. G. P. Korchemsky and S. Tafat, J. High Energy Phys. **0010**, 010 (2000)
18. L. V. Yakushevich, *Nonlinear Physics of DNA, Wiley* (2004).